

Plasticin, a Type III Neuronal Intermediate Filament Protein, Assembles as an Obligate Heteropolymer: Implications for Axonal Flexibility

*William S. Asch and *†‡Nisson Schechter

*Department of Biochemistry and Cell Biology; †Department of Psychiatry and Behavioral Science, Health Sciences Center; and ‡Institute for Cell and Developmental Biology, State University of New York, Stony Brook, New York, U.S.A.

Abstract: The assembly characteristics of the neuronal intermediate filament protein plasticin were studied in SW13 cells in the presence and absence of a cytoplasmic filament network. Full-length plasticin cannot polymerize into homopolymers in filament-less SW13c1.2Vim⁻ cells but efficiently coassembles with vimentin in SW13c1.1Vim⁻ cells. By cotransfecting plasticin and vimentin in SW13c1.1Vim⁻ cells, we show that plasticin assembly requires vimentin in noncatalytic amounts. Differing effects on assembly were seen with point mutations of plasticin monomers that were analogous to the keratin mutations that cause epidermolysis bullosa simplex (EBS). In particular, plasticin monomers with point mutations analogous to those in EBS do not uniformly inhibit neurofilament (NF) network formation. A point mutation in the helix termination sequence resulted in complete filament aggregation when coexpressed with vimentin but showed limited coassembly with low- and medium-molecular-weight NF proteins (NF-L and NF-M, respectively). In transfected SW13c1.1Vim⁺ cells, a point mutation in the first heptad of the α -helical coil region formed equal amounts of filaments, aggregates, and a mixture of filaments and aggregates. Furthermore, coexpression of this point mutation with NF-L and NF-M was associated with a shift toward increased numbers of aggregates. These results suggest that there are important structural differences in assembly properties between homologous fish and mammalian intermediate filament proteins. These structural differences may contribute to the distinctive growth characteristics of the teleost visual pathway.

Key Words: Neurofilament—Zebrafish—Cytoskeleton—Axonogenesis.

J. Neurochem. **75**, 1475–1486 (2000).

The zebrafish visual pathway, like the goldfish visual pathway, has a remarkable capacity for continuous growth throughout life (Johns and Easter, 1977; Meyer, 1978; Marcus et al., 1999). In response to injury, most, if not all, goldfish optic axons regenerate and restore functional connections with their tectal targets (Attardy and Sperry, 1963; Sperry, 1963). Although goldfish have been studied more intensively, recent evidence suggests that the zebrafish is likely to have a similar response to

injury (Bernhardt et al., 1996; Asch et al., 1998; Marcus et al., 1999).

We have used the goldfish and zebrafish visual pathways to identify proteins that show altered expression in response to optic nerve injury with the goal of identifying specific proteins that support the growth process (Glasgow et al., 1992, 1994; Asch et al., 1998). In particular, two intermediate filament (IF) proteins (IFPs), plasticin and gefiltin, show a dramatic and sequential increase in expression in retinal ganglion cells, with plasticin preceding gefiltin following optic nerve crush (Glasgow et al., 1994; Asch et al., 1998). Moreover, in the retinal ganglion cell layer of normal goldfish, plasticin and gefiltin are expressed in an age-related pattern: Plasticin is only expressed in the youngest cells, whereas gefiltin is found in the mature cells (Fuchs et al., 1994; Glasgow et al., 1994; Asch et al., 1998). This suggests that plasticin functions during the initial stages of retinal ganglion cell axonogenesis, whereas gefiltin functions during the later stages of the growth process. It is noteworthy that the sequential expression of plasticin and gefiltin during development and, following optic nerve crush, is reminiscent of the developmental expression of their mammalian homologues, peripherin and α -internexin (Escurat et al., 1990; Troy et al., 1990; Fliegner et al., 1994). Thus, we propose that these developmentally regulated IFPs have structural attributes that support

Received April 12, 2000; revised manuscript received May 11, 2000; accepted May 11, 2000.

Address correspondence and reprint requests to Dr. N. Schechter at Department of Psychiatry and Behavioral Science, Health Sciences Center, T-10, State University of New York, Stony Brook, NY 11794-8101, U.S.A. E-mail: nschechter@mail.psychiatry.sunysb.edu

Abbreviations used: EBS, epidermolysis bullosa simplex; FITC, fluorescein isothiocyanate; HA, hemagglutinin; IF, intermediate filament; IFP, intermediate filament protein; mAb, monoclonal antibody; NF-H, NF-L, and NF-M, heavy-, light-, and medium-molecular-weight neurofilament protein, respectively; NFP, neurofilament protein; pAb, polyclonal antibody; PBS, phosphate-buffered saline; PBS-T, 1× phosphate-buffered saline, 3% goat serum, and 0.1% Triton X-100; TRITC, tetramethylrhodamine isothiocyanate.

the staged growth of optic axons during development and regeneration.

Although plasticin was originally discovered in the teleost visual pathway, it is also transiently expressed in other neurons during zebrafish development (Canger et al., 1998). In particular, plasticin expression is detected in restricted subsets of projection neurons that pioneer distinct axon tracts in the embryo. These developmental studies further indicate that plasticin has structural attributes that subservise the morphology of the neuron during its early growth phase.

Structurally, plasticin is a type III IFP (Geisler et al., 1983). As such, it has specific amino acid sequences and a structural organization that is similar to those of other cytoplasmic IFPs. To determine whether the plasticin protein can influence the organization of an IF network and, if so, determine which regions of the protein contribute, we turned to the keratins, another IFP type for which significant structure–function information is available.

In humans, keratin mutations are associated with diseases such as epidermolysis bullosa simplex (EBS) and epidermolytic hyperkeratosis (reviewed by Coulombe, 1993). Although the exact mechanism is unclear, mutant keratin monomers disrupt keratin networks by interfering with some stage of the assembly process. Extensive studies on filament assembly *in vitro* suggest that something goes awry during the progression from tetramers to protofilaments during polymerization (Letai et al., 1992). Most of the natural point mutations recovered to date suggest that interactions between adjacent α -helices are affected (Chan et al., 1996). Of usefulness to plasticin function studies in zebrafish is the dominant-negative action these mutant keratin subunits possess. They are able to pair with endogenous subunits to form the lower-order dimeric and tetrameric structures but are unable to assemble into higher-order structures (Fuchs and Coulombe, 1992). Thus, these mutant subunits can effectively draw normal subunits out of the monomer pool and prevent their assembly into filamentous structures (Fuchs and Coulombe, 1992). However, despite the highly conserved nature of the α -helical coil domain, we could not assume that all IFPs with equivalent mutations will behave like keratin. Nonetheless, these disease-producing keratin mutations provide methodological insights into studies of IFP structure and function during neurogenesis.

We engineered cDNAs that encode plasticin monomers having point mutations that are homologous to two of the mutant keratin K14 genes, commonly found in patients with EBS. Preliminary microinjection studies, using mRNA transcribed from these cDNAs *in vitro*, showed gross developmental defects in some injected zebrafish embryos. However, these defects were difficult to interpret because it was not known whether plasticin would promiscuously coassemble into nonneuronal IF networks. Furthermore, our preliminary studies did not allow us to follow transgenic protein that was ectopically expressed after microinjection. Before plasticin microin-

jection studies in zebrafish embryos could be interpreted, a detailed analysis in a defined cellular environment was needed.

SW13 cells offer a unique cellular context in which IF assembly can be assessed. The mosaic expression of vimentin, the only cytoplasmic IF expressed in SW13 cells, was first recognized by Hedberg and Chen (1986). Subsequently, highly related subcultures of SW13 cells were isolated based on the presence or absence of vimentin expression (Sarria et al., 1994). Although these cultures are not pure, they do provide an experimental cell system that is virtually free of cytoplasmic IF expression. Thus, the assembly properties of wild-type and mutant IF subunits can be determined in isolation or in the context of IF reconstituted cells (Cui et al., 1995; Sun et al., 1997; Ching and Liem, 1999).

In this report, we show that plasticin, unlike its mammalian homologue peripherin, is unable to form a homopolymeric IF network in SW13 cells. Rather, plasticin forms dense cellular aggregates in cells lacking an IF cytoskeleton. However, plasticin does polymerize to form an IF network in vimentin-containing cells. Furthermore, plasticin subunits bearing EBS point mutations at the end of the α -helical coil domain show assembly defects in the presence of vimentin, but, surprisingly, vimentin polymerization is apparently not affected to the same degree. Moreover, the plasticin point mutation at the beginning of the α -helical coil domain is largely rescued by cotransfection with the low- and medium-molecular-weight neurofilament proteins (NFPs) (NF-L and NF-M, respectively).

MATERIALS AND METHODS

Cell culture

Human adrenal carcinoma SW13 c1.1Vim⁺ and SW13 c1.2Vim⁻ cells were generously provided by Dr. Robert Evans (University of Colorado Health Sciences Center, Denver, CO, U.S.A.). Cells were grown in a 1:1 mixture of Dulbecco's modified Eagle's medium and Ham's F12 (GibcoBRL, Gaithersburg, MD, U.S.A.) supplemented with 5% fetal bovine serum, 100 U/ml penicillin G sodium, and 100 μ g/ml streptomycin sulfate. All cells were maintained at 37°C, or 32°C where noted, in a humidified atmosphere supplemented with 5% CO₂.

DNA constructs

Mutations in plasticin (Asch et al., 1998) were generated by *in vitro* mutagenesis using the method described by Kunkel (1985). In brief, plasmids were transformed into the *Escherichia coli* strain CJ236 to yield single-stranded, uracil-containing circular DNA using the M13K07 helper phage. Single-stranded plasmid was purified from the helper phage by preparative gel electrophoresis. Phosphorylated oligonucleotides containing internal mutations (synthesized by Genosys Biotechnologies, The Woodlands, TX, U.S.A.) were hybridized to the single-stranded plasmid and extended with T7 DNA polymerase. The resulting double-stranded plasmid was transformed into *E. coli* strain XL1-Blue MRF' (Stratagene, La Jolla, CA, U.S.A.). Appropriate mutations were identified by sequencing DNA obtained from mini-preps (RPM kit; Bio 101, Vista, CA, U.S.A.) as described previously (Asch et al., 1998). All plasticin cDNAs were subsequently cloned as *Hind*III–

EcoRI fragments into pBluescript P/X HA3 (Neiman et al., 1997) using standard PCR techniques. These plasticin-hemagglutinin (HA) tag fusion cDNAs were then cloned as *HindIII*-*XbaI* fragments into the mammalian expression vector pcDNA3.1 (Invitrogen, San Diego, CA, U.S.A.). Untagged plasticin cDNAs were cloned as *EcoRI*-*XbaI* fragments into pCS2+ (Rupp et al., 1994; Turner and Weintraub, 1994) using standard PCR techniques. Plasmids used for transfection were purified using the Plasmid Maxi Kit (Qiagen, Hilden, Germany). The pRSVi-NF-L, pRSVi-NF-M, and pRSVi-vimentin expression constructs (Chin and Liem, 1989; Sun et al., 1997) were generously provided by Dr. Ronald H. K. Liem (Columbia University College of Physicians and Surgeons, New York, NY, U.S.A.). The VimGG+D expression construct (Beuttenmuller et al., 1994) was kindly provided by Drs. Peter Traub and Robert Shoeman (Max Planck Institute for Cell Biology, Ladenburg, Germany).

DNA transient transfections

SW13 cells were transfected using the nonliposomal lipid formulation Fugene 6 (Boehringer Mannheim Biochemicals, Indianapolis, IN, U.S.A.) according to the manufacturer's instructions. In brief, 18 h before transfection, cells were split and plated into 35-mm-diameter culture dishes that contained a sterile 22-mm square coverslip. Cells were grown overnight to ~30% confluence. DNA was complexed with Fugene 6 at a ratio of 1:3 ($\mu\text{g}:\mu\text{l}$) in 100 μl of serum-free Dulbecco's modified Eagle's medium for 15 min and added directly to the overnight cultures. Cells were allowed to grow under the transfection conditions for an additional 24–36 h, after which they were fixed for immunocytochemistry. All transfections were repeated a minimum of two times.

Antibodies

The anti-plasticin (clone CL3) polyclonal antibody (pAb) has been described previously (Fuchs et al., 1994) and was used at a dilution of 1:1,000 for immunohistochemistry. The anti-vimentin monoclonal antibody (mAb) was used at a dilution of 1:100 (clone V9; Sigma Chemical Co., St. Louis, MO, U.S.A.). The anti-NF-L and anti-NF-M mAbs (clones NR4 and NN18, respectively) were also obtained from Sigma and used at a dilution of 1:250. The anti-HA mAb (clone 12CA5; Boehringer Mannheim Biochemicals) was used at 1.6 $\mu\text{g}/\text{ml}$. Secondary antibodies included goat anti-mouse IgG1 pAb conjugated with fluorescein isothiocyanate (FITC), goat anti-mouse IgG2b pAb conjugated with tetramethylrhodamine isothiocyanate (TRITC), goat anti-rabbit IgG (heavy and light chain) pAb conjugated with FITC, and goat anti-rabbit IgG (heavy and light chain) pAb conjugated with TRITC. The goat anti-mouse pAbs were used at a dilution of 1:500. The goat anti-rabbit pAbs were used at a dilution of 1:250. Secondary antibodies were obtained from Southern Biotechnology Associates (Birmingham, AL, U.S.A.). All antibodies were diluted in phosphate-buffered saline (PBS) supplemented with 3% serum.

Immunocytochemistry

Following transfection, cultures were rinsed three times with PBS (deficient in Ca^{2+} and Mg^{2+}) and then fixed in cold methanol for 10 min at -20°C . After four 5-min washes with PBS, the cells were blocked for 30 min in PBS supplemented with 3% serum. Cells were subsequently washed with PBS and incubated with primary antibody for 1 h at room temperature with gentle shaking. To remove unbound primary antibody, cells were washed four times with PBS for 5 min. Cells were then incubated with secondary antibody for 30 min in the dark

at room temperature with gentle shaking. Cells were once again washed four times with PBS for 5 min to remove unbound secondary antibody. Coverslips were mounted wet, using 12 μl of aqueous antifade solution {10 mg/ml diazabicyclo[2.2.2]octane (Sigma), 90% glycerol, and $1\times$ PBS, pH 8.6}, and sealed using conventional nail polish. Cells were stored in the dark overnight at room temperature and viewed using a $95\times$ fluorescence objective (Leitz, Wetzlar, Germany) on an IMT-2 inverted fluorescence microscope equipped with a PM-30 exposure control unit (Olympus, Melville, NY, U.S.A.). All images were captured on Ektachrome 400 positive film (Eastman Kodak, Rochester, NY, U.S.A.) and scanned into a personal computer (Dell Computer, Round Rock, TX, U.S.A.) using a SprintScan 35 Plus (Polaroid, Cambridge, MA, U.S.A.) slide scanner. Images were captured at the highest resolution possible (2,700 dpi) and processed using Photoshop (version 4.0; Adobe Systems, San Jose, CA, U.S.A.).

Cell extractions and immunoblot analysis

Cell extracts from 100-mm-diameter plates were prepared, as previously described (Ching and Liem, 1993), using 2 ml of lysis buffer. Proportional amounts of the Triton X-100-insoluble fraction from SW13c1.1Vim⁺ and SW13c1.2Vim⁻ cells were electrophoresed in sodium dodecyl sulfate-10% polyacrylamide gels and were electrotransferred to polyvinylidene difluoride membranes. Membranes were blocked overnight in PBS containing 0.1% Triton X-100 and 5% powdered milk. The CL3 pAb was used at a dilution of 1:5,000 in PBS-T ($1\times$ PBS, 3% goat serum, and 0.1% Triton X-100) for western blots. The goat anti-rabbit alkaline phosphatase-conjugated secondary antibody (Sigma) was used at 1:10,000 in PBS-T. The blot was developed using the NBT (nitro blue tetrazolium) and BCIP (5-bromo-4-chloro-3-indolyl phosphate) alkaline phosphatase substrates (GibcoBRL) and processed as described above.

RESULTS

Plasticin is unable to form normal homopolymeric IF networks in SW13 cells

Transfection of mammalian expression constructs into SW13c1.2Vim⁻ cells is a reliable system for assessing the homopolymer-forming properties of IFPs. Therefore, we determined whether zebrafish plasticin can assemble to form a cytoplasmic IF network, in the absence of any other IFPs, by introducing plasmid pCS2+PlastB-ORF (Fig. 1) into SW13c1.2Vim⁻ cells using the nonliposomal lipid formulation Fugene 6. After 24–36 h of incubation, cells were fixed, and plasticin expression was visualized by fluorescence immunohistochemistry using the CL3 pAb. Nonfilamentous aggregates were found in nearly all of the fluorescently labeled cells (Fig. 2A). Typically, aggregates varied in size between cells as well as within a single cell. This staining pattern is distinct from the diffuse staining that would be likely in the presence of stable monomers. Furthermore, these aggregations are not soluble in 1% Triton X-100, indicating that filament assembly may have proceeded beyond tetrameric structures (Fig. 3). Very rarely, a cell could be found that demonstrated plasticin homopolymer assembly. Because 1% of cells in SW13c1.2Vim⁻ cultures express vimentin (Sarría et al., 1994), cells that contained

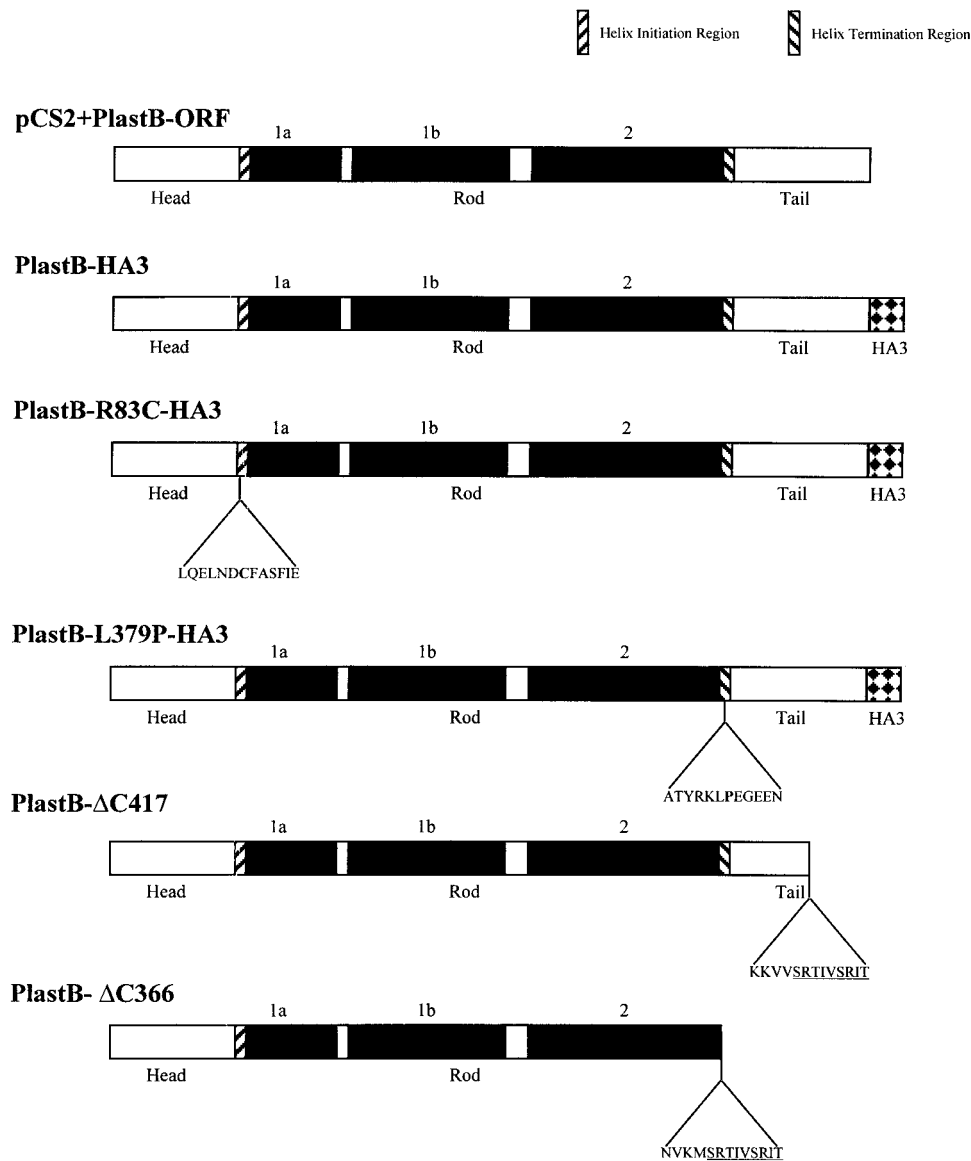


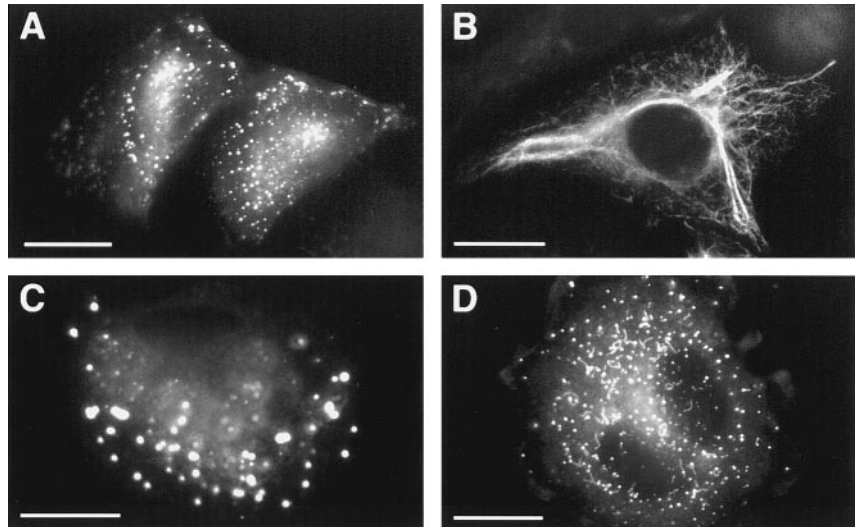
FIG. 1. Schematic illustration of the full-length, point mutation, and deletion plasticin constructs used in these studies. The locations of head, rod, and tail domains and HA3 epitope tags are indicated. Amino acid sequences in the vicinity of the point mutations are shown with the one-letter code, and the mutated amino acid is shown in bold. Amino acid sequences at the deletion junctions are also shown, and additional amino acid residues generated during cloning are underlined. Note that the PlastB-ΔC417 construct is truncated before the RGD sequence and that the PlastB-ΔC366 construct is truncated 5' of the KLEGEE sequence.

plasticin filaments were most likely vimentin-expressing mosaic cells in the SW13c1.2Vim⁻ culture. These results indicated that wild-type plasticin is unable to polymerize into homopolymeric IFs but would be able to heteropolymerize with vimentin. Indeed, when pCS2+plasticin was transfected into SW13c1.2Vim⁺, plasticin protein assembled into the filamentous architecture characteristic of IFs (Fig. 2B).

At 37°C, trout, *Xenopus*, and zebrafish vimentins are unable to self-assemble to form normal filamentous networks in cultured cells (Herrmann et al., 1993, 1996; Cerda et al., 1998). However, this assembly defect is temperature-dependent because IF polymerization oc-

curs when cultures are cooled below 34°C (Cerda et al., 1998). To determine whether plasticin self-assembly is similarly temperature-dependent, we transiently transfected and cultured SW13c1.2Vim⁻ cells with pCS2+PlastB-ORF at 32°C. SW13 cells grown for 24 h at 32°C displayed normal morphology and did not release from the culture plate. No visual difference between these cells and SW13 cells grown at 37°C was apparent. In nearly all cells, we observed diffuse cytoplasmic staining and filament aggregation (Fig. 2C). Rarely, we identified a cell in which plasticin polymerized into extremely short, disconnected structures (Fig. 2D). Because plasticin did not homopolymerize at 32°C,

FIG. 2. Immunofluorescence of SW13 cells transiently transfected with pCS2+ORF. **A:** Plasticin is unable to form a normal filamentous homopolymer in SW13c1.2Vim⁻ cells. **B:** Plasticin is able to coassemble with vimentin in SW13c1.1Vim⁺ cells. The inability of plasticin to self-assemble in SW13c1.2Vim⁻ cells is not a function of the assembly temperature. **C:** Plasticin is unable to self-assemble in SW13c1.2Vim⁻ cells at 32°C. **D:** In rare cases, plasticin polymerized into extremely short, disconnected structures in SW13c1.2Vim⁻ cells at 32°C. Bar = 20 μm.



a temperature predicted to be permissive for zebrafish filament assembly, its self-assembly is not temperature-dependent under the conditions described here.

Plasticin assembly is unimpeded by addition of the HA tag to the carboxy terminus

Our studies in developing zebrafish embryos use an epitope-tagged form of plasticin to discriminate between expression of endogenous and microinjected plasticin. An added advantage of epitope tagging is that plasticin can be visualized immunohistochemically, yet antibody cross-reactivity with similar IFPs is eliminated. To visualize microinjected plasticin protein, three tandem copies of the HA antigen epitope were inserted, in frame, at the C terminus. The resulting clones were further subcloned into the expression vector pcDNA3.1 and expressed *in vitro* to ensure that the clones produced full-length, in-frame proteins (data not shown). When PlastB_{HA3} (Fig. 1) is introduced into SW13 cells, the results are identical to those obtained with pCS2+PlastB-ORF, namely, plasticin is able to form normal-appearing IF networks in cells expressing vimentin (Fig. 4A) but is unable to self-assemble in vimentin-free cells (Fig. 4B). Thus, addition of the triple HA tag does not impede plasticin filament coassembly with vimentin. Furthermore, using dual labeling of SW13c1.2Vim⁺ cells, it is clear that PlastB_{HA3} coassembles with vimentin to form filament networks (Fig. 4C and D). Attempts to tag plasticin with the c-myc and FLAG epitopes at the N terminus blocked

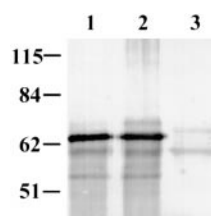
assembly in vimentin-positive SW13 cells (authors' unpublished data).

The requirement of vimentin for assembly is not catalytic

Having determined that plasticin can form filament networks in SW13c1.2Vim⁺ but not SW13c1.2Vim⁻ cells, we investigated whether catalytic quantities of vimentin are sufficient for coassembly. Vimentin-free SW13 cells were cotransfected with plasticin and vimentin expression constructs at varying molar ratios but with a fixed total amount of transfected plasmid. When cotransfected at a ratio of 100:1 (plasticin:vimentin) all of the cells formed aggregates (Fig. 5A). However, when the amount of vimentin is increased to a ratio of 100:10, a clear difference in staining is observed (Fig. 5B). Plasticin is still aggregated in about half of the transfected cells. The other half of the cells show plasticin forming spherical cytoplasmic aggregates that are often in connection with some short, loosely packed filamentous structures. These aggregates were of a smaller size when compared with those typically formed by cotransfecting plasticin with vimentin at a ratio of 100:1 in SW13c1.2Vim⁻ cells. This "ball and chain" phenotype was previously reported using point mutations of vimentin, namely, VimKK+D and VimKR+D (Beuttenmuller et al., 1994). However, little is known about the assembly dynamics that produce these structures. When plasticin and vimentin expression plasmids are cotransfected at equivalent molar levels, the phenotype is still different (Fig. 5C). These cells have cytoplasmic IF networks that vary in density and length. Some are loosely packed like the filaments formed at the 100:10 ratio, but others resemble normal IF networks. Similarly, some of the filaments are very short, whereas others appear to be of normal length.

Having determined that plasticin assembly is qualitatively dose-dependent but not reliant on vimentin in catalytic amounts, we sought to determine whether plas-

FIG. 3. Immunoblot of the Triton X-100-insoluble fractions from SW13 cells. Following transient transfection in SW13c1.2Vim⁻ (lane 1) and SW13c1.1Vim⁺ (lane 2) cells, plasticin is found in the Triton X-100-insoluble fraction. The plasticin CL3 pAb was used for detection. The cell extract of nontransfected SW13c1.1Vim⁺ cells was used as a negative control (lane 3).



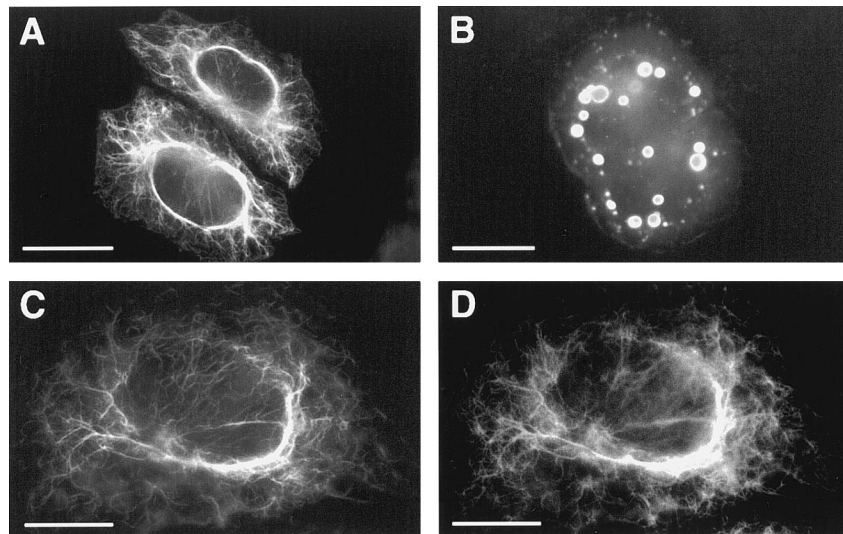


FIG. 4. Addition of the HA3 epitope tag does not alter the assembly properties of plasticin in SW13 cells. $\text{PlastB}_{\text{HA3}}$ forms normal filaments in SW13c1.1Vim⁺ cells (A) but is unable to self-assemble in SW13c1.2Vim⁻ cells (B). A dual-labeling immunofluorescence assay shows that $\text{plastB}_{\text{HA3}}$ (C) colocalizes with vimentin (D) in SW13c1.1Vim⁺ cells. Bar = 20 μm .

ticin assembly requires vimentin assembly or whether some other structural feature of vimentin could be involved. For example, the vimentin “head,” alone, might be sufficient for the plasticin assembly process, even if vimentin itself is unable to assemble. To determine whether threshold amounts of vimentin or a subdomain of vimentin is required, even in the absence of vimentin assembly, we cotransfected equivalent quantities of $\text{PlastB}_{\text{HA3}}$ with the assembly-defective vimentin expression vector VimGG+D (Beuttenmuller et al., 1994). Analysis of these cells showed that plasticin does not assemble even with addition of high quantities of an assembly-defective vimentin subunit (Fig. 5D). Thus, it appears that the ability of plasticin to coassemble in vimentin-containing cells depends on the ability of vimentin to assemble. Furthermore, this dependence is not catalytic in that small quantities of assembly-competent vimentin cannot lead to complete plasticin polymerization.

Carboxyl-terminally truncated plasticin protein is able to form IF networks in SW13c1.1Vim⁺

Carboxyl-terminal deletion mutants of NF-L and NF-M show a dominant-negative effect on the assembly of vimentin in cultured mouse fibroblast L cells. Similarly, expression of tailless peripherin mutants in SW13c1.1Vim⁺ cells disrupted the entire vimentin IF network. However, this has not been a universal property of all IFs. For example, carboxyl-terminal deletion mutants of desmin had no detectable impairment of polymerization. To determine whether plasticin mutants would behave like desmin or like NF-L, NF-M, and peripherin, we transfected SW13c1.1Vim⁺ cells with a carboxyl-terminal deletion mutant of plasticin, $\text{PlastB-}\Delta\text{C366}$ (Fig. 1). This construct does not contain the region against which the plasticin antibody was raised, and we did not want to confound the carboxyl-terminal deletion analysis by adding a carboxyl-terminal HA tag. Consequently, we visualized $\text{PlastB-}\Delta\text{C366}$ filament networks via copolymer-

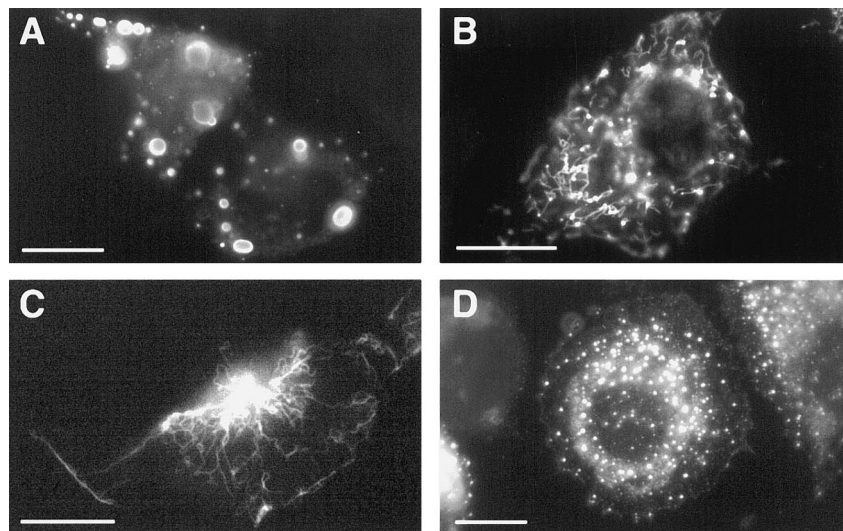
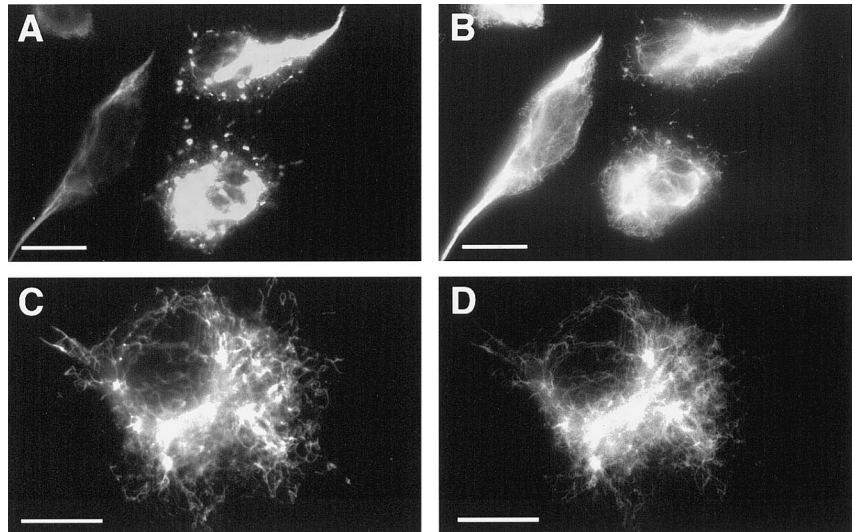


FIG. 5. The requirement of vimentin for plasticin assembly is not catalytic. **A:** Cotransfection of plasticin ($\text{PlastB}_{\text{HA3}}$) and vimentin at a ratio of 100:1, respectively, produced aggregates in SW13c1.2Vim⁻ cells. **B:** Cotransfection at a ratio of 10:1 resulted in both filament formation and aggregation, with some cells having filaments with a “ball and chain” appearance. **C:** When equimolar quantities of plasticin and vimentin expression constructs were cotransfected, the cytoplasmic IF networks produced varied in filament length and density. **D:** Cotransfection of equimolar amounts of plasticin and assembly-defective VimGG+D expression constructs does not result in coassembly. Bar = 20 μm .

FIG. 6. Coassembly of C-terminal deletion mutants of plasticin with vimentin. **A:** Deletion of the entire tail and helix termination sequence renders plasticin unable to coassemble with vimentin. **B:** Furthermore, vimentin assembly is adversely affected. Deletion of the plasticin tail up to, but not including, the RDG motif does not alter coassembly of plasticin (**C**) and vimentin (**D**) in most cells. Bar = 20 μm .



ization with trace amounts of PlastB_{HA3} using the anti-HA mAb. Without the entire tail and helix termination sequence from coil 2b, PlastB- Δ C366 is unable to form normal filament networks in transfected cells (Fig. 6A). Furthermore, the aggregates that formed in these SW13c1.1Vim⁺ cells contained plasticin and most of the vimentin in the cell (Fig. 6B). Therefore, PlastB- Δ C366 is unable to coassemble with vimentin and also interferes with vimentin assembly in a dominantly negative fashion. However, PlastB- Δ C417, a plasticin cDNA that encoded a subunit that contained the tail up to but not including the type III tail RDG motif (Fig. 1), was able to polymerize with vimentin and form normal IF networks in the majority of cells analyzed (Fig. 6C). Furthermore, PlastB- Δ C417 was able to coassemble normally with vimentin (Fig. 6D). Thus, the conserved helix termination sequence KLEEGEE is required for proper coassembly of plasticin with vimentin, whereas the conserved RDG region is not.

Plasticin bearing EBS-like point mutations R83C and L379P have aberrant filament-forming properties

A possible means of interfering with plasticin function is by blocking its ability to assemble properly. Therefore, we engineered point mutations analogous to those found in the keratin K14 gene of patients with EBS. This was possible because these mutations are found in the keratin rod, a highly conserved domain among IFPs (Steinert and Roop, 1988). Mutations that alter the normal charge arrangement in the rod domain heptad repeats might alter the packing of filaments, either within a filament or between adjacent filament structures (Chan et al., 1996). In particular, we made two constructs: The first is an R/C conversion at amino acid position 83 (analogous to R125C in human K14); the second is an L/P conversion at amino acid position 379 (analogous to L384P in human K14). The EBS phenotype produced by the L384P

mutation is characteristically less severe than that of the R125C mutation (reviewed by Fuchs and Coulombe, 1992). These engineered cDNAs were also cloned in frame with HA tags (Fig. 1).

PlastB-R83C_{HA3} has a variable phenotype when transfected into SW13c1.2Vim⁺. This is surprising as extrapolation of keratin K14 studies predicted that this mutation should be extremely resistant to filament formation. The variable phenotype is characterized by three unique presentations, each represented equally among the transfected cells: Cells have plasticin aggregates, normal filaments, or a mixture of the two together (Fig. 7A–C). It is even more surprising that when dual labeling is used to covisualize vimentin, we see filaments that are normal in the majority of cells. Furthermore, in those cells where plasticin has formed nonfilamentous aggregates, vimentin is primarily filamentous (compare Fig. 7A and D). Occasionally, we found a cell that had aggregated plasticin but a decreased density of vimentin filaments. Immunohistochemistry depicts a fixed point in the time course of the assembly process. Therefore, in these cells it is not possible to distinguish whether vimentin was being expressed at normal levels and later down-regulated as a result of PlastB-R83C_{HA3} expression or expressed at levels below normal independent of PlastB-R83C_{HA3} expression. Nevertheless, assembly-defective plasticin R83C subunits do not appear to act definitively in a dominant-negative fashion. Rather, it appears that they are largely recessive to vimentin's assembly characteristics.

Unlike PlastB-R83C_{HA3}, which has a variable phenotype in SW13c1.2Vim⁺ cells, PlastB-L379P_{HA3} is universally unable to assemble. Immunostaining shows that all cells transfected with PlastB-L379P_{HA3} have filament aggregates (Fig. 7F). Furthermore, many of the cells with aggregates have clear perikaryal aggregates with a "strand of pearls" presentation (Fig. 7E). It is interesting

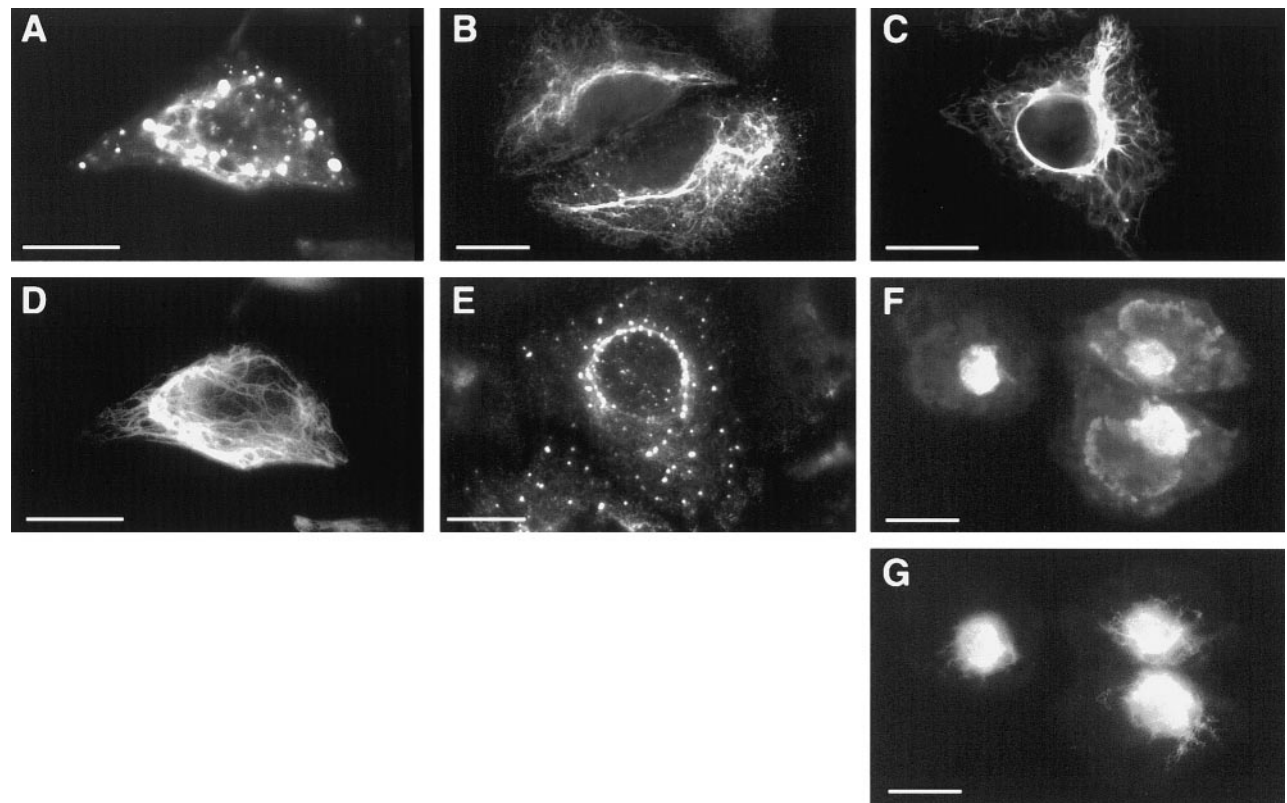


FIG. 7. EBS-like point mutations affect the assembly of plasticin with vimentin and the NFPs. Expression of PlastB-R83C_{HA3} results in cells having (A) total aggregation, (C) normal filaments, or (B) a mixture of the two extremes. D: Furthermore, dual labeling shows that vimentin assembles normally in these cells. E: Expression of PlastB-L379P_{HA3} with vimentin resulted in filament aggregation, sometimes with perikaryal clustering. Dual labeling shows that when PlastB-L379P_{HA3} aggregates (F), vimentin assembly is aberrant (G). Bar = 20 μ m.

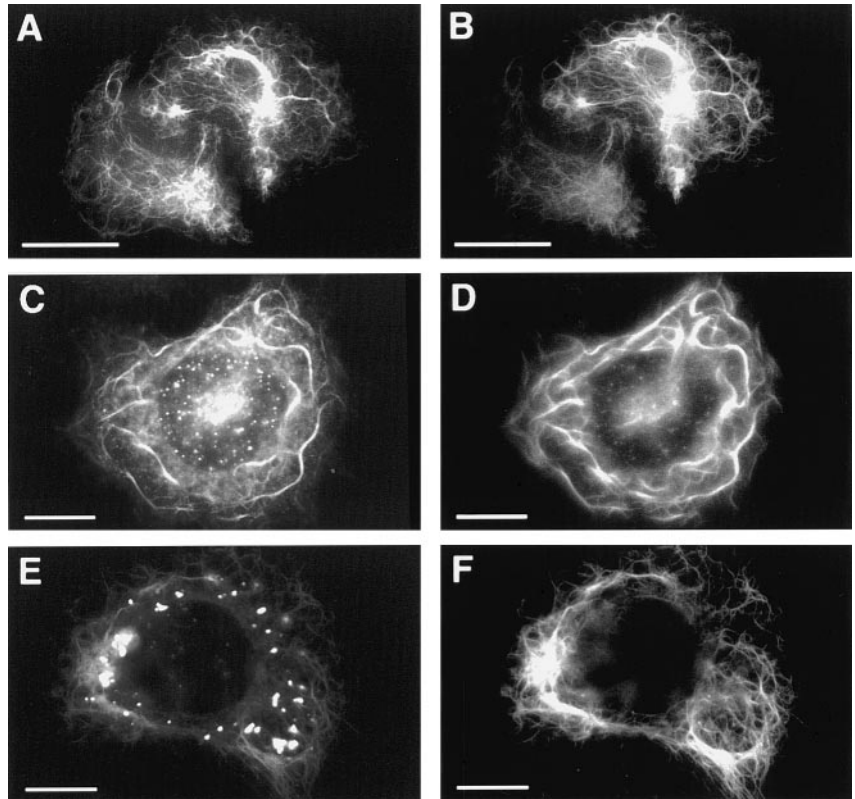
that despite the presence of plasticin aggregates, some normal vimentin staining can be seen but usually emanating from an aggregate (Fig. 7G). Thus, PlastB-L379P_{HA3} assembly is completely incompetent in SW13c1.2Vim⁺ cells and causes a severe disruption in endogenous vimentin polymerization.

Plasticin point mutants R83C and L379P have contextual phenotypes in SW13 cells

Having assessed the filament-forming capacities of plasticin point mutations PlastB-R83C_{HA3} and PlastB-L379P_{HA3} in SW13c1.2Vim⁺ cells, we characterized the filament-forming properties of these mutant filaments in SW13c1.2Vim⁻ cells that were reconstituted with an NF-L and NF-M IF network. We chose to study the assembly properties of plasticin in the context of an NF-L/NF-M heteropolymer because this environment is more likely to replicate the cellular environment of plasticin expression. In particular, following optic nerve crush both NF-L and NF-M are present during the period of increased plasticin expression. The large-molecular-weight NFP (NF-H) was omitted from these studies because it was never detected in teleost optic nerve (Quitschke et al., 1985). All three constructs were co-

transfected at a ratio of 2:1:1 (plasticin:NF-L:NF-M). The results from immunostaining show a phenotype different from that seen when the plasticin mutations were coassembled with vimentin. Cotransfections of SW13c1.2Vim⁻ cells with constructs encoding PlastB-R83C_{HA3}, NF-L, and NF-M resulted in staining that indicated an increased number of cytoplasmic aggregates when compared with the transfections of PlastB-R83C_{HA3} in SW13c1.1Vim⁺ cells (compare Figs. 7A–C and 8C and D). Furthermore, unlike the complete aggregation that occurs when PlastB-L379P_{HA3} is coexpressed with vimentin, coexpression of PlastB-L379P_{HA3} with NF-L and NF-M primarily results in aggregation with some cells displaying both aggregation and low levels of filament formation (Fig. 8E and F). Because the two mutant constructs behaved differently, i.e., an increased filament-forming ability was observed for PlastB-L379P_{HA3}, whereas plastB-R83C_{HA3} showed a decrease, we do not think that the altered assembly characteristics are a result of dissimilar expression levels between single transfection of SW13c1.1Vim⁺ and triple cotransfection of SW13c1.1Vim⁻ cells. Finally, normal plasticin efficiently coassembles with NF-L and NF-M into filamentous networks (Fig. 8A and B).

FIG. 8. When cotransfected with NF-L and NF-M into SW13c1.2Vim⁻, the assembly defects of PlastB-R83C_{HA3} and PlastB-L379P_{HA3} differ from those seen with vimentin coassembly in SW13c1.1Vim⁺ cells. As a control, PlastB_{HA3} can coassemble with (A) NF-L and (B) NF-M in SW13c1.2Vim⁻ cells. C: Coexpression of PlastB-R83C_{HA3}, NF-L, and NF-M results in more consistent filament aggregation than PlastB-R83C_{HA3} expression in SW13c1.1Vim⁺ cells. D: Furthermore, dual labeling shows that NF-L and NF-M assembly is not significantly affected. E: Coexpression of PlastB-L379P_{HA3} shows primarily filament aggregation but also some filamentous structures. F: Unlike PlastB-L379P_{HA3} expression in SW13c1.1Vim⁺ cells, dual labeling shows that NF-L and NF-M assemble normally when cotransfected with PlastB-L379P_{HA3}. Bar = 20 μm.



DISCUSSION

Using cultured SW13 cells we demonstrate that the assembly properties of plasticin differ in several respects from those of other type III IF proteins. In particular, plasticin is the first member of the type III IF class that fails to assemble as a homopolymer. This is in contrast to the mammalian homologue of plasticin, peripherin, which is capable of self-assembly into a normal filament network in SW13c1.2Vim⁻ cells (Cui et al., 1995). This suggests either that the ability of peripherin to form a homopolymeric network is not essential to its function, or that peripherin evolved to serve a cellular process different from plasticin. Moreover, although the developmental expression patterns of plasticin, peripherin, and XIF3 are similar, there are significant differences. For example, XIF3 is expressed in the neuroectoderm, whereas plasticin and peripherin are not (Sharpe et al., 1989; Gervasi et al., 2000). Thus, although it can be argued that the functional attributes of plasticin, peripherin, and XIF3 each support similar but unique structural requirements in their respective species, it is tempting to speculate that some of the functional attributes have also changed. The inability of plasticin to form a homopolymer may be one aspect of this divergence.

Although there is increasing evidence that plasticin and peripherin are orthologues (Gervasi et al., 2000), dissimilarity in their ability to form homopolymers may be primarily a reflection of the differences in their amino acid sequences, particularly at the amino terminus. Ze-

brafish and goldfish plasticins have shortened head domains when compared with peripherin (Asch et al., 1998). It is this region of the protein that is strategic for the self-assembly of other IFPs, namely, vimentin (Herrmann et al., 1992; Beuttenmuller et al., 1994), desmin (van den Heuvel et al., 1987), NF-L (Gill et al., 1990), NF-M (Wong and Cleveland, 1990), and NF-H (Sun et al., 1997). Furthermore, plasticin has only a partial match, SYR, to the highly conserved nonapeptide sequence SSSYRRIFGG common to type III IFPs in the head region (Asch et al., 1998). Although a precise function has not been attributed to this sequence, it is likely to play a role in the self-assembly process. Point mutations in this region block self-assembly of vimentin (Herrmann et al., 1992; Beuttenmuller et al., 1994), as does replacement of the entire head domain with the green fluorescent protein (Ho et al., 1998). Furthermore, vimentin amino-terminal truncations and point mutations are unable to coassemble with normal vimentin, whereas green fluorescent protein–vimentin can coassemble with normal vimentin (Ho et al., 1998). Another hypothesis is that the uninterrupted coil I region of NF-M and NF-H prevents their assembly in the absence of an NF-L “backbone” (reviewed by Nixon and Shea, 1992). This is not the case for plasticin, which, like NF-L, has an interrupted coil I domain.

Mammalian cultured cells at lower temperatures are permissive for IFP assembly. For example, Herrmann et al. (1993) transfected *Xenopus* vimentin into a bovine

mammary gland epithelial cell line at 28°C. In contrast to 37°C, this lower temperature was permissive for *Xenopus* vimentin assembly. We chose to transfect plasticin into SW13 cells at 32°C, a temperature well within the permissive range of normal zebrafish physiology, and closer to normal mammalian physiological temperatures than is 28°C. Because plasticin was unable to assemble at 32°C, it is not likely that the inability of plasticin to self-assemble in SW13c1.2Vim⁻ cells is a temperature-dependent phenomenon. This is in contrast to zebrafish vimentin, which has minimal self-assembly at 37°C but polymerizes into a normal filamentous network at temperatures between 28 and 34°C. The inability of plasticin to self-assemble at 32°C can be attributed to differences in the primary structure of plasticin when compared with other type III IFPs, particularly, vimentin. Of the 13 amino acids likely to be mediating this temperature sensitivity (Herrmann et al., 1993, 1996), six show clear homology between plasticin and vimentin. However, of these six amino acids only one is divergent between plasticin and peripherin, which self-assembles at 37°C (Cui et al., 1995).

Glial fibrillary acidic protein is also a type III IFP and, like plasticin, lacks the SSYRRIFGG sequence. However, glial fibrillary acidic protein does have a comparable serine- and arginine-rich region at its amino terminus (Herrmann et al., 1992) and, unlike plasticin, is able to self-assemble into a filamentous network in SW13c1.2Vim⁻ cells (Chen and Liem, 1994). When this serine- and arginine-rich region is deleted, glial fibrillary acidic protein loses its capacity for self-assembly. This finding emphasizes the importance of higher structural levels rather than strict conservation of the canonical sequence motif in this region. Despite this ability of glial fibrillary acidic protein to self-assemble in culture, abnormal filaments result from self-assembly in vivo. Specifically, the astrocytes of vimentin null mice form abnormally compact glial fibrillary acidic protein filament bundles presumably because the noncanonical serine-arginine-rich motif of glial fibrillary acidic protein has become insufficient for normal self-assembly (Pekny et al., 1999). Nonetheless, it is conceivable that the weak serine-arginine character of this region could permit plasticin self-assembly in vivo in zebrafish even though it is insufficient for plasticin assembly in SW13c1.2Vim⁻ cells.

Unexpectedly, plasticin point mutations analogous to those found in the keratin genes of patients with EBS are not definitive dominant-negatives with regard to assembly. Because plasticin is unable to form a normal homopolymeric network, the effects of these point mutations on plasticin networks are impossible to assess. However, networks formed from the coassembly of PlastB-R83C_{HA} with vimentin show a mixed distribution of aggregated and filamentous structures. Thus, it would appear that the assembly capacity of vimentin is, at least in part, sufficient to rescue the assembly incompetence of PlastB-R83C_{HA}. This suggests that alignment of plasticin and vimentin during assembly does not depend on

contacts within the first heptad of plasticin. Because plasticin has no proline or glycine in the "pre-rod" domain and has putative heptad repeats with the appropriate hydrophobic residues, it is possible that the pre-rod domain of the type III proteins already adopts an α -helical structure before the start of the "true rod" (Quax-Jeuken et al., 1983). Such a structural configuration could permit plasticin R83C to form "normal" filaments in contrast to similar mutations in keratins. In contrast to the networks formed when PlastB-R83C_{HA} coassembles with vimentin, coassembly of PlastB-R83C_{HA3} with NF-L and NF-M in SW13c1.1Vim⁻ cells resulted in more frequent filament aggregations. Thus, the assembly of plasticin with the NFPs appears to be more dependent on subunit interactions within the first "true" heptad than is the assembly of plasticin with vimentin.

PlastB-L379P_{HA} was uniformly unable to assemble in SW13c1.1Vim⁺ cells. Here, too, we see a contextual assembly phenotype. When cotransfected with the NFP expression constructs, there was a slight shift toward normal filament assembly; however, the majority of cells still showed filament aggregation. Therefore, PlastB-L379P_{HA3}, with its altered helix termination sequence, has a similar and only slightly less detrimental effect on filament assembly as the truncation mutant PlastB- Δ C366, which lacks the helix termination sequence completely.

Consistent with NF-L and NF-M studies (Gill et al., 1990; Wong and Cleveland, 1990; Chin et al., 1991), a carboxyl-terminal deletion mutant of plasticin that removes the entire tail region, PlastB- Δ C366, behaves as a dominant-negative with regard to vimentin assembly. However, a longer plasticin subunit that contained the tail region up to, but not including, the RDG consensus motif has the capacity to copolymerize. Thus, in plasticin the KLLGEE motif, which is thought to restrict the α -helical turns within the rod region, is required for normal filament assembly. Moreover, our results are consistent with previous studies that have demonstrated that the RDG tripeptide is not required for monomer incorporation into existing filament networks (Makarova et al., 1994). However, because plasticin does not self-assemble normally, it is impossible to determine whether homopolymerization requires the RDG tripeptide.

Although a precise function of NFPs has not been determined, they appear to act in an architectural capacity much like keratin in the epidermis and desmin in the myocardium (reviewed by Galou et al., 1997). Examination of axonal caliber in the quail mutant *Quiver*, as well as in several transgenic mice, led to the hypothesis that NFPs are determinants of axonal caliber (reviewed by Lee and Cleveland, 1996). Furthermore, axonal caliber and conduction velocity are directly linked (Gasser and Erlanger, 1927). NF-L-null mice, which showed a decreased axonal caliber, also had a decreased conduction velocity (Zhu et al., 1997). Therefore, the assembly of the neurofilament network bears on the electrophysiological properties of neurons.

The assembly characteristics of plasticin, together with the timing of expression, suggest that this protein alters the physiological properties of the neurofilament network. In particular, its expression rises during the early stages of axonal regeneration while the NFPs are being down-regulated (Oblinger et al., 1989). Furthermore, it seems to be a weak molecule with regard to assembly as both vimentin and the NFPs are able to rescue partially a proposed dominant-negative form of the protein. Moreover, based on our studies here, plasticin could never successfully form a filamentous architecture by itself. Thus, it appears unlikely that plasticin plays a structural role in a manner that increases IF network rigidity. Rather, we speculate that plasticin plays a novel role by increasing the flexibility of the neurofilament network.

Plasticin expression may be a physiological strategy for increasing axonal flexibility while still providing some minimal degree of cytoskeletal support. Such a function would be particularly advantageous during development and regeneration, when environmental demands on elongating neurons require increased axonal plasticity.

Acknowledgment: We thank Dr. R. Liem (Columbia University) for providing the NF-L, NF-M, and vimentin constructs, Drs. P. Traub and R. Shoeman (Max-Planck-Institut für Zellbiologie) for providing the VimGG+D construct, and Dr. N. Dean (State University of New York at Stony Brook) for providing the HA tag fusion construct. We thank Dr. R. Evans (University of Colorado Health Sciences Center) for providing the SW13 cell lines used in this study. Special thanks to Dr. M. Evinger (State University of New York at Stony Brook) for allowing us to use her fluorescence microscopy equipment. We also thank Dr. L. Fochtman for a critical reading of the manuscript. This work was supported by grant EY05212 from the National Institutes of Health (to N.S.).

REFERENCES

- Asch W. S., Leake D., Canger A. K., Passini M. A., Argenton F., and Schechter N. (1998) Molecular cloning of the zebrafish neurofilament proteins plasticin and gefiltin: increased mRNA expression in ganglion cells after optic nerve crush. *J. Neurochem.* **71**, 20–32.
- Attardy D. G. and Sperry R. W. (1963) Preferential selection of central pathways by regenerating optic fibers. *Exp. Neurol.* **7**, 46–64.
- Bernhardt R. R., Tongiorgi E., Anzini P., and Schachner M. (1996) Increased expression of specific recognition molecules by retinal ganglion cells and by optic pathway glia accompanies the successful regeneration of retinal axons in adult zebrafish. *J. Comp. Neurol.* **376**, 253–264.
- Beuttenmuller M., Chen M., Janetzko A., Kuhn S., and Traub P. (1994) Structural elements of the amino-terminal head domain of vimentin essential for intermediate filament formation in vivo and in vitro. *Exp. Cell Res.* **213**, 128–142.
- Canger A. K., Passini M. A., Asch W. S., Leake D., Zafonte B. T., Glasgow E., and Schechter N. (1998) Restricted expression of the neuronal intermediate filament protein plasticin during zebrafish development. *J. Comp. Neurol.* **399**, 561–572.
- Cerda J., Conrad M., Markl J., Brand M., and Herrmann H. (1998) Zebrafish vimentin: molecular characterization, assembly properties and developmental expression. *Eur. J. Cell Biol.* **77**, 175–187.
- Chan Y.-M., Cheng J., Gedde-Dahl T. J., Niemi K.-M., and Fuchs E. (1996) Genetic analysis of a severe case of Dowling-Meara epidermolysis bullosa simplex. *J. Invest. Dermatol.* **106**, 327–334.
- Chen W. J. and Liem R. K. (1994) The endless story of the glial fibrillary acidic protein. *J. Cell Sci.* **107**, 2299–2311.
- Chin S. S. M. and Liem R. K. H. (1989) Expression of rat neurofilament proteins NF-L and NF-M in transfected non-neuronal cells. *Eur. J. Cell Biol.* **50**, 475–490.
- Chin S. S., Macioce P., and Liem R. K. (1991) Effects of truncated neurofilament proteins on the endogenous intermediate filaments in transfected fibroblasts. *J. Cell Sci.* **99**, 335–350.
- Ching G. Y. and Liem R. K. (1993) Assembly of type IV neuronal intermediate filaments in nonneuronal cells in the absence of preexisting cytoplasmic intermediate filaments. *J. Cell Biol.* **122**, 1323–1335.
- Ching G. Y. and Liem R. K. H. (1999) Analysis of the roles of the head domains of type IV rat neuronal intermediate filament proteins in filament assembly using domain-swapped chimeric proteins. *J. Cell Sci.* **112**, 2233–2240.
- Coulombe P. A. (1993) The cellular and molecular biology of keratins: beginning a new era. *Curr. Opin. Cell Biol.* **5**, 17–29.
- Cui C. Q., Stambrook P. J., and Parysek L. M. (1995) Peripherin assembles into homopolymers in SW13 cells. *J. Cell Sci.* **108**, 3279–3284.
- Escurat M., Djabali K., Gumpel M., Gros F., and Portier M.-M. (1990) Differential expression of two neuronal intermediate-filament proteins, peripherin and the low-molecular-mass neurofilament protein (NF-L), during development in rat. *J. Neurosci.* **10**, 764–784.
- Fliegner K. H., Kaplan M. P., Wood T. L., Pintar J. E., and Liem R. K. H. (1994) Expression of the gene for the neuronal intermediate filament protein alpha-internexin coincides with the onset of neuronal differentiation in the developing rat nervous system. *J. Comp. Neurol.* **342**, 161–173.
- Fuchs E. and Coulombe P. A. (1992) Of mice and men: genetic skin diseases of keratin. *Cell* **69**, 899–902.
- Fuchs C., Glasgow E., Hitchcock P. F., and Schechter N. (1994) Plasticin, a newly identified neurofilament protein, is preferentially expressed in young retinal ganglion cells of adult goldfish. *J. Comp. Neurol.* **350**, 452–462.
- Galou M., Gao J., Humbert J., Mericskay M., Li Z., Paulin D., and Vicart P. (1997) The importance of intermediate filaments in the adaptation of tissues to mechanical stress: evidence from gene knockout studies. *Biol. Cell* **89**, 85–97.
- Gasser H. S. and Erlanger J. (1927) The role played by the sizes of the constituent fibers of nerve trunk in determining the form of its action potential wave. *Am. J. Physiol.* **80**, 522–547.
- Geisler N., Kaufman E., Fischer S., Plessman U., and Weber K. (1983) Neurofilament architecture combines structural principles of intermediate filaments with carboxy-terminal extensions increasing in size between triplet proteins. *EMBO J.* **2**, 1295–1302.
- Gervasi C., Stewart C.-B., and Szaro B. G. (2000) *Xenopus laevis* peripherin (XIF3) is expressed in radial glia and proliferating neural epithelial cells as well as in neurons. *J. Comp. Neurol.* **423**, 512–531.
- Gill S. R., Wong P. C., Monteiro M. J., and Cleveland D. W. (1990) Assembly properties of dominant and recessive mutations in the small mouse neurofilament (NF-L) subunit. *J. Cell Biol.* **111**, 2005–2019.
- Glasgow E., Druger R. K., Levine E. M., Fuchs C., and Schechter N. (1992) Plasticin, a novel type III neurofilament protein from goldfish retina: increased expression during optic nerve regeneration. *Neuron* **9**, 373–381.
- Glasgow E., Druger R. K., Fuchs C., Lane W. S., and Schechter N. (1994) Molecular cloning of gefiltin (ON1): serial expression of two new neurofilament mRNAs during optic nerve regeneration. *EMBO J.* **13**, 297–305.
- Hedberg K. K. and Chen L. B. (1986) Absence of intermediate filaments in a human adrenal cortex carcinoma derived cell line. *Exp. Cell Res.* **163**, 509–517.
- Herrmann H., Hofmann I., and Franke W. W. (1992) Identification of a nonapeptide motif in the vimentin head domain involved in intermediate filament assembly. *J. Mol. Biol.* **223**, 637–650.
- Herrmann H., Eckelt A., Brettel M., Grund C., and Franke W. W. (1993) Temperature-sensitive intermediate filament assembly. Al-

- ternative structures of *Xenopus laevis* vimentin in vitro and in vivo. *J. Mol. Biol.* **234**, 99–113.
- Herrmann H., Munick M. D., Brettel M., Fouquet B., and Markl J. (1996) Vimentin in a cold-water fish, the rainbow trout: highly conserved primary structure but unique assembly properties. *J. Cell Sci.* **109**, 569–578.
- Ho C. L., Martys J. L., Mikhailov A., Gundersen G. G., and Liem R. K. (1998) Novel features of intermediate filament dynamics revealed by green fluorescent protein chimeras. *J. Cell Sci.* **111**, 1767–1778.
- Johns P. R. and Easter S. S. Jr. (1977) Growth of the adult goldfish eye. II. Increase in retinal cell number. *J. Comp. Neurol.* **176**, 331–341.
- Kunkel T. A. (1985) Rapid and efficient site-specific mutagenesis without phenotypic selection. *Proc. Natl. Acad. Sci. USA* **82**, 488–492.
- Lee M. K. and Cleveland D. W. (1996) Neuronal intermediate filaments. *Annu. Rev. Neurosci.* **19**, 187–217.
- Letai A., Coulombe P. A., and Fuchs E. (1992) Do the ends justify the mean? Proline mutations at the ends of the keratin coiled-coil rod segment are more disruptive than internal mutations. *J. Cell Biol.* **116**, 1181–1195.
- Makarova I., Carpenter D., Khan S., and Ip W. (1994) A conserved region in the tail domain of vimentin is involved in its assembly into intermediate filaments. *Cell Motil. Cytoskeleton* **28**, 265–277.
- Marcus R. C., Delaney C. L., and Easter S. S. Jr. (1999) Neurogenesis in the visual system of embryonic and adult zebrafish (*Danio rerio*). *Vis. Neurosci.* **16**, 417–424.
- Meyer R. L. (1978) Evidence from thymidine labeling for continuing growth of retina and tectum in juvenile goldfish. *Exp. Neurol.* **59**, 99–111.
- Neiman A. M., Mhaiskar V., Manus V., Galibert F., and Dean N. (1997) *Saccharomyces cerevisiae* HOC1, a suppressor of pkc1, encodes a putative glycosyltransferase. *Genetics* **145**, 637–645.
- Nixon R. A. and Shea T. B. (1992) Dynamics of neuronal intermediate filaments: a developmental perspective. *Cell Motil. Cytoskeleton* **22**, 81–91.
- Oblinger M. M., Wong J., and Parysek L. M. (1989) Axotomy-induced changes in the expression of a type III neuronal intermediate filament gene. *J. Neurosci.* **9**, 3766–3775.
- Pekny M., Johansson C. B., Eliasson C., Stakeberg J., Wallen A., Perlmann T., Lendahl U., Betsholtz C., Berthold C.-H., and Frisen J. (1999) Abnormal reaction to central nervous system injury in mice lacking glial fibrillary acidic protein and vimentin. *J. Cell Biol.* **145**, 503–514.
- Quax-Jeuken Y. E., Quax W. J., and Bloemendal H. (1983) Primary and secondary structure of hamster vimentin predicted from the nucleotide sequence. *Proc. Natl. Acad. Sci. USA* **80**, 3548–3552.
- Quitschke W., Jones P. S., and Schechter N. (1985) Survey of intermediate filament proteins in optic nerve and spinal cord: evidence for differential expression. *J. Neurochem.* **44**, 1465–1476.
- Rupp R. A. W., Snider L., and Weintraub H. (1994) *Xenopus* embryos regulate the nuclear localization of XMyoD. *Genes Dev.* **8**, 1311–1323.
- Sarria A. J., Lieber J. G., Nordeen S. K., and Evans R. M. (1994) The presence or absence of a vimentin-type intermediate filament network affects the shape of the nucleus in human SW-13 cells. *J. Cell Sci.* **107**, 1593–1607.
- Sharpe C. R., Pluck A., and Gurdon J. B. (1989) XIF3, a *Xenopus* peripherin gene, requires an inductive signal for enhanced expression in anterior neural tissue. *Development* **107**, 701–714.
- Sperry R. W. (1963) Chemoaffinity in the orderly growth of nerve fiber patterns and connections. *Proc. Natl. Acad. Sci. USA* **50**, 703–710.
- Steinert P. M. and Roop D. R. (1988) Molecular and cellular biology of intermediate filaments. *Annu. Rev. Biochem.* **57**, 593–625.
- Sun D. M., Macioce P., Chin S. S. M., and Liem R. K. H. (1997) Assembly properties of amino- and carboxyl-terminally truncated neurofilament NF-H proteins with NF-L and NF-M in the presence and absence of vimentin. *J. Neurochem.* **68**, 917–926.
- Troy C. M., Muma N. A., Greene L. A., Price D. L., and Shelanski M. L. (1990) Regulation of peripherin and neurofilament expression in regenerating rat motor neurons. *Brain Res.* **529**, 232–238.
- Turner D. L. and Weintraub H. (1994) Expression of achaete-scute homolog 3 in *Xenopus* embryos converts ectodermal cells to a neural fate. *Genes Dev.* **8**, 1434–1447.
- van den Heuvel R. M., van Eys G. J., Ramaekers F. C., Quax W. J., Vree Egberts W. T., Schaart G., Cuypers H. T., and Bloemendal H. (1987) Intermediate filament formation after transfection with modified hamster vimentin and desmin genes. *J. Cell Sci.* **88**, 475–482.
- Wong P. C. and Cleveland D. W. (1990) Characterization of dominant and recessive assembly-defective mutations in mouse neurofilament NF-M. *J. Cell Biol.* **111**, 1987–2003.
- Zhu Q., Couillard-Despres S., and Julien J.-P. (1997) Delayed maturation of regenerating myelinated axons in mice lacking neurofilaments. *Exp. Neurol.* **148**, 299–316.